Relationship Between Funduscopic Conus and Optic Disc Factors Associated with Myopia in Young Healthy Eyes

Hiroto Terasaki, Takehiro Yamashita, Minoru Tanaka, Kumiko Nakao, and Taiji Sakamoto

Department of Ophthalmology, Kagoshima University Graduate School of Medical and Dental Sciences, Kagoshima, Japan

Correspondence: Taiji Sakamoto, Department of Ophthalmology, Kagoshima University Graduate School of Medical and Dental Sciences, Kagoshima, Japan; tsakamot@m3.kufm.kagoshima-u.ac.jp.

Received: June 28, 2019
Accepted: November 14, 2019
Published: February 25, 2020

Citation: Terasaki H, Yamashita T, Tanaka M, Nakao K, Sakamoto T. Relationship between funduscopic conus and optic disc factors associated with myopia in young healthy eyes. *Invest Ophthalmol Vis Sci.* 2020;61(2):40. https://doi.org/10.1167/iovs.61.2.40

Purpose. To determine the relationship between funduscopic findings in myopic eyes and the prevalence and structure of the conus in the optical coherence tomographic (OCT) images.

Methods. A prospective observational cross-sectional study of 121 right eyes of 121 young healthy volunteers. All participants underwent color fundus photography (CFP), scanning laser ophthalmoscopy, and OCT. Based on the OCT analyses, the area between the edge of the ellipsoid zone (EZ) and that of choroid was defined as the "choroidal conus (CC)", and the area between the edge of the choroid and the scleral edge as the "scleral conus (SC)". The eyes were classified into three groups such as the non-conus (NC) group, CC group, and SC group. The differences in the axial length, optic disc tilt, ovality ratio, papillomacular position angle, and peripapillary nerve fiber elevation (pNFE) between the three groups were determined.

Results. CFPs detected a conus in 79 eyes (65.3 %). The outer border of the conus in CFPs corresponded with the edge of the EZ in the OCT in all subjects. Thirty-seven eyes had CC alone (CC group) and 42 eyes had both CC and SC (SC group). The CC and SC groups had longer axial lengths and more frequent pNFEs than the NC group. There was a significant difference in the optic disc tilt and ovality ratio between the CC and SC groups.

Conclusions. The eyes with SC tend to have larger optic disc tilt and smaller ovality ratio than the eyes with CC only.

Keywords: choroid structure, myopic conus, peripapillary atrophy

The incidence of myopia is increasing across the world and is becoming a major medical and social problem.[1,2] Although myopia is an important ocular disorder that can cause glaucoma and chorioretinal atrophy,[3–5] the mechanisms causing its development has not been definitively determined. In addition, the treatment and prevention of myopia have not been adequately addressed. Thus it is important to study the mechanisms involved in the development of myopia to be able to examine and treat it effectively.

One of the characteristic findings of the fundus of myopic eyes is the presence of a myopic conus.[6] The myopic conus is generally recognized as a grayish or whitish area on the temporal side of the optic nerve in the fundus photographs (Fig. 1). Earlier, similar findings in the eyes of glaucoma patients were called peripapillary atrophies (PPAs).[7] The PPAs are divided into the α zone, β zone, and γ zone by their anatomic locations. Jonas et al.[7] examined histological images and concluded that the α zone of PPAs is an irregular pigmented area just lateral to its border with the β zone, the β zone is an area between the end of Bruch's membrane (BM) and the beginning of the retinal pigment epithelium (RPE), and the γ zone is the area between the end of BM and the outer margin of the optic nerve. In 2013, Dai et al.[8] proposed a new subclassification of PPA based on optical coherence tomographic (OCT) findings. OCT based β zone PPA has been described as an area where the RPE is absent, but BM is present. Gamma zone PPA is described as an area where both RPE and BM areas are absent.[8] It has been recently reported that the presence of a β zone was a risk factor for glaucoma progression,[9] and the eyes with greater width of the γ zone have significantly larger visual field defects compared with the fellow eyes.[10]

Because the classification of coni was originally made by examinations of color fundus photographs, we believed that it was important to continue using this method. Tokoro and Ohno[11] reported that examining the conus in the fundus photographs showed that there were cases in which the conus could be divided into two regions: the choroidal conus (CC) and scleral conus (SC, Fig. 1). Our preliminary analyses of OCT B-scan images showed that the boundary between these two areas coincided with the edge of the choroid. Because a conus is a common finding in myopic eyes, we believed that coni may be involved in the pathogenesis and progression of myopia. However, the incidence of the two types of coni and their relationships with other parameters of myopic eyes have not been determined.

Thus the purpose of this study was to determine the incidence of the two types of coni, and to compare the myopic parameters of eyes with these two types of coni. To reduce the effects of age and pathological changes, we examined the conus of young adults whose growth and myopic changes were stabilized.

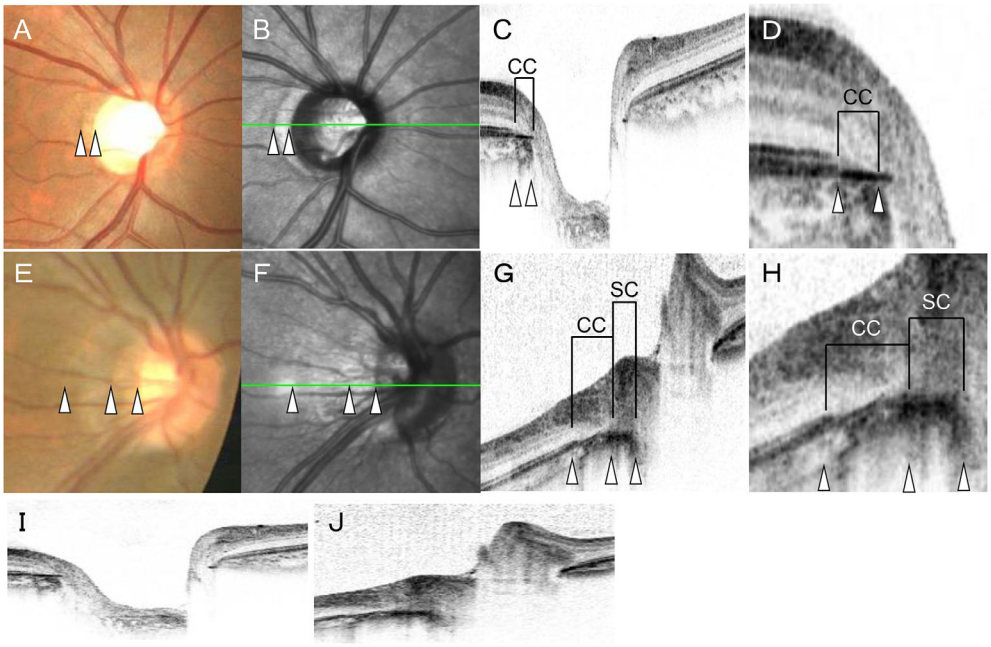

Figure 1. CC and SC determined by OCT. Upper: An eye with a CC (A-D, I). Lower: An eye with both choroidal and scleral coni (E-H, J). White triangles are corresponding positions to the fundus photographs (A, E), scanning laser ophthalmoscopy (SLO) images (B, F), cross-sectional OCT images (C, G), and the magnified OCT images (D, H). The Y-scale of the OCT image was 1:1 pixel in C, D, G, and H, and 1:1 micrometer in I and J. Color fundus photographs show that there are two types of coni in a healthy eye. One has a uniform color tone in the conus as in the upper photograph, and the other has a color tone similar to that in the upper eye and a whitish area along the optic nerve. OCT B-scan shows that the conus in the upper case corresponds to the area between the edge of the choroid along with the optic disc and the stump of the ellipsoid zone (CC). In the lower case, there was CC and the conus where the sclera was exposed along the optic disc (SC).

Methods

Ethics Statement

All of the procedures used conformed to the tenets of the Declaration of Helsinki. A written informed consent was obtained from all of the subjects after an explanation of the procedures to be used. The study was approved by the Ethics Committee of Kagoshima University Hospital, and it was registered with the University Hospital Medical Network (UMIN)-clinical trials registry. The registration title was, "Morphological analysis of the optic disc and the retinal nerve fiber in myopic eyes" and the registration number was UMIN000006040. A detailed protocol is available at https://upload.umin.ac.jp/cgi-open-bin/ctr/ctr.cgi?function=brows&action=brows&type=summary&recptno=R000007154&language=J.

Subjects

This was a cross-sectional, observational study. We initially examined 133 eyes of 133 volunteers who were enrolled between November 1, 2010, and February 29, 2012. The volunteers had no known eye diseases as determined by examining their medical charts, and the data from only the right eyes were analyzed. The eligibility criteria were age ≥20 years but ≤40 years; eyes normal by slit-lamp biomicroscopy, ophthalmoscopy, and OCT; the best-corrected visual acuity ≤0.1 logarithm of the minimum angle of resolution (logMAR) units; and intraocular pressure (IOP) ≤21 mmHg. The exclusion criteria were eyes with known ocular diseases such as glaucoma, staphyloma, and optic disc anomaly; known systemic diseases such as hypertension and diabetes; presence of visual field defects; and prior refractive or intraocular surgery. None of the eyes were initially excluded because of poor OCT image quality caused by poor fixation. Three eyes were excluded due to a superior segmental optic disc hypoplasia, one eye was excluded due to a glaucoma, and three eyes were excluded because of prior refractive surgery. Five other eyes were excluded because of difficulty in assessing the conus. In the end, the right eyes of 121 individuals were used for the statistical analyses.

Measurement of Axial Length and Refractive Error

All eyes had a standard ocular examination, including slit-lamp biomicroscopy of the anterior segment, ophthalmoscopy of the ocular fundus, pneumotonometric (CT-80, Topcon, Tokyo, Japan) measurements of the IOP, and AL-2000 ultrasonographic (Tomey, Nagoya, Japan) measurements of the axial length. The refractive error (spherical equivalent) was measured with the Topcon KR8800 autorefractometer/keratometer.

Measurements of Optic Disc by OCT

Color fundus photographs were taken with the TRC-50LX (Topcon). Scanning laser ophthalmoscopy (SLO) images and optic disc cross-sectional images were taken with Spectralis OCT (Heidelberg Engineering, Heidelberg, Germany). The scan pattern was centered on the optic nerve head with a raster pattern of 73 horizontal B-scan spanning 15 degrees without EDI-OCT method. The data for each B-scan were averaged from seven individual B-scans. The operator

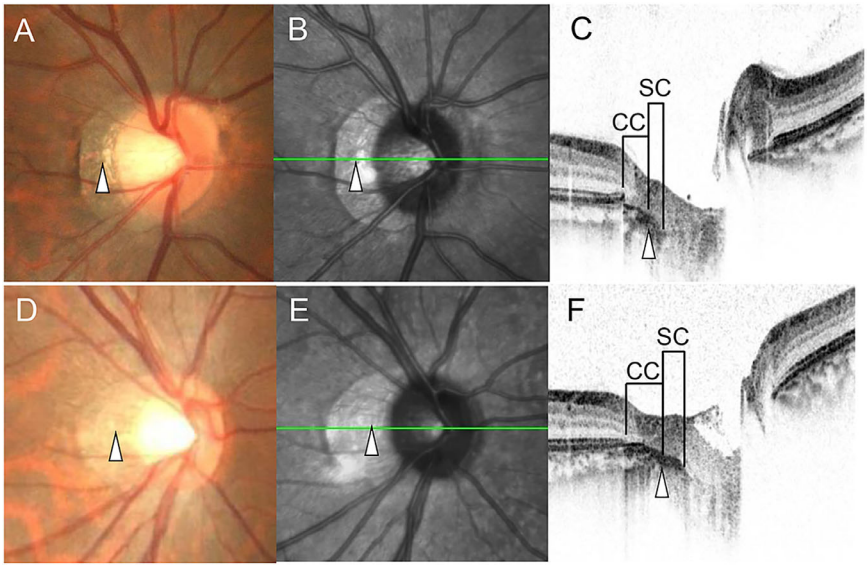

Figure 2. Detection of the CC and SC in color fundus photographs and SLO images. Upper: A, B, and C are eyes with a visible border between the CC and SC. Lower: D, E, and F are eyes with no detectable border between CC and SC. White triangles are corresponding positions of the border between CC and SC in the fundus photographs (A, D), scanning laser ophthalmoscopic images (B, E), and cross-sectional OCT images (C, F). The Y-scale of the OCT image was 1:1 pixel.

checked for image quality, including whether the SD-OCT B-scan position was correct in the image frame, centered on the optic nerve head (ONH), and quality score >20. When necessary, images were reacquired. Positional alignment of the color fundus ophthalmoscopic and SLO fundus images was done using Photoshop software (Adobe, San Jose, CA, USA) based on the vascular pattern. Then the positional adjustments of the SLO and color fundus images and the OCT cross-sectional images were made using Spectralis OCT software.

Assessments for Existence of Myopic Conus in Color Fundus Photographs

The presence of a conus was determined by confirming the presence of a parapapillary crescent in the color fundus photographs by two independent examiners (TY and MT). The assessments of the conus were made by the two raters independently. If the raters disagreed, the eye was excluded from the study. Five eyes were excluded because of the disagreement on the presence of a conus between the two masked raters.

Detection of Border Between Choroidal and Scleral Edge

We determined whether the outer border of the conus in the color fundus photographs was coincident with the end of the ellipsoid zone in the OCT images (Fig. 1). Based on the OCT findings, the area between the edge of the ellipsoid zone and the edge of the choroid was defined as 'choroidal conus' (CC) and the area between the edge of the choroid and scleral edge as the 'scleral conus' (SC). Then we determined the prevalence of the CC and SC, and the visibility of the border between the CC and the SC in the color fundus and SLO photographs (Fig. 2). This analysis was performed by two independent examiners (TY and MT). If the results did not match, the final classification and subclassification were decided in discussions with a third rater (HT).

Determination of Papillomacular Position (PMP), Ovality Ratio, and Optic Disc Tilt

Color fundus photographs and OCT images were taken at the same time with the Topcon 3D OCT-1000 Mark II (Topcon). The PMP is the angle formed by a horizontal line and a line connecting the optic disc center and the fovea on the color fundus photographs.[12] The ovality ratio was determined on the color fundus photographs as described in detail.[13] The maximum and minimum disc diameters were measured by a single observer using Photoshop software. We defined the vertically axis of the disc as the longest diameter that was less than 45 degrees of the geometric vertical axis, and the horizontal axis as the longest diameter that was more than 45 degrees of the geometric vertical axis. The ovality ratio was determined by dividing the minimum by the maximum disc diameters. The degree of the optic disc tilt was quantified as we have reported.[13] Briefly, the optic disc tilt was quantified using a sine curve method of the Topcon 3D OCT-1000 Mark II RNFL 3.4-mm circle scan, B scan images (Topcon). The course of the RPE was marked on the B-scan images manually. The coordinates of each pixel were determined automatically using ImageJ software (http://imagej.nih.gov/ij/; provided in the public domain by the National Institutes of Health, Bethesda, MD, USA). The x and y coordinates of the B-scan images were converted to a new set of x and y coordinates with the center of the wave as the origin. Finally, the converted data were fit to a sine wave equation ($y = \alpha \times \sin(b \times x - c)$) with the curve fitting program of ImageJ. The amplitude of the sine curve a was defined as the degree of the optic disc tilt. We had

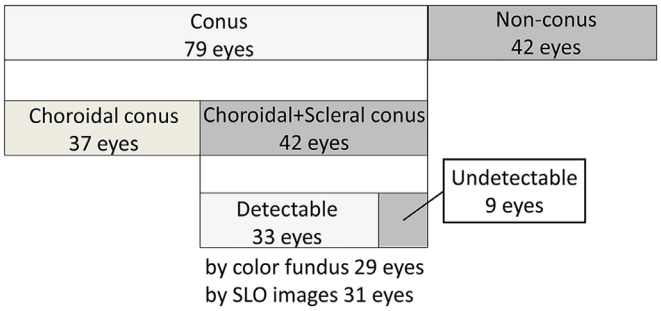

Figure 3. Classification of CC and SC.

shown the high intratater and interrater repeatability of this method previously.[13]

Assessments of Peripapillary Nerve Fiber Elevation (pNFE)

The pNFE is the elevation of the nerve fiber layer, which is frequently observed in the nasal peripapillary area of the optic disc.[14] The presence of the pNFE was determined by examining the color fundus photographs, SLO images, and optic disc cross-sectional OCT images. The definition of a pNFE was a white-colored tissue similar to the optic disc rim by ophthalmoscopy, tissue on the optic disc rim with a clear inner margin but no clear outer margin by SLO, and an elevated tissue continuous with the optic disc with the same reflectivity as the ganglion cell-inner plexiform layer.

Statistical Analyses

All statistical analyses were performed with SPSS statistics 21 for Windows (IBM Corp., Armonk, NY, USA), and the statistical programming language R (version 3.0.2, The R Foundation for Statistical Computing, Vienna, Austria). The Kruskal-Wallis 1-way analysis of variance and the Steel-Dwass multiple comparison tests and the Fisher's exact test were used to determine the significant differences of the age, sex, axial lengths, optic disc tilt, ovality ratio, PMP, and pNFE among the non-conus (NC) group, CC group, and SC group.

Results

Classification of NC, CC, and SC

There were 42 eyes (34.7 %) without a myopic conus, and 79 eyes (65.3 %) with a myopic conus. In eyes with a myopic conus, 37 eyes (46.8 %) had a CC alone, and 42 eyes (53.1%) had a combination of a CC and SC. All of the eyes with SC had a CC. In all 79 eyes, the lateral edge of the conus corresponded with the edge of ellipsoid zone. In the SC group, the border between the CC and the SC was detected in 33 eyes (78.6 %): 29 eyes in the color fundus photographs and 31 eyes in the SLO images. It was difficult to detect the border in the other 9 eyes (21.4 %) (Fig. 3).

There were 42 eyes (34.7 %) without a myopic conus, and 79 eyes (65.3 %) with a myopic conus. In eyes with a myopic conus, 37 eyes (46.8 %) had a CC alone, and 42 eyes (53.1%) had a combination of a CC and SC. All of the eyes with SC had a CC. In all of the 79 eyes, the lateral edge of the conus corresponded with the edge of ellipsoid zone. In the SC group, a border between the CC and the SC was detected in 33 eyes (78.6 %), with 29 eyes of these in the color fundus photographs and 31 eyes in the SLO images. It was difficult to detect the border in the other 9 eyes (21.4%).

Comparison of Ocular Parameters in NC, CC, and SC Groups

The characteristics of the eyes in the NC, CC, and SC groups are shown in the Table. Among the 121 eyes of myopic subjects (less than –0.5 diopter), there were 66.7% (28/42 eyes) of the individuals in the NC group, 97.3% (36/37 eyes) in the CC group, and 100.0% (42/42 eyes) in the SC group. The age was not significantly different among the three groups ($P = 0.79$). The sex distribution was also not significantly different among the three groups (NC vs. CC group; $P = 0.47$, CC vs. SC group; $P = 1.00$, NC vs. SC group; $P = 0.48$). The refractive error of the NC group (–2.35 ± 3.38 D) was significantly greater than that of the CC group (–5.37 ± 3.00 D; $P < 0.001$) and the SC group (–6.19 ± 2.53 D; $P < 0.001$). There was no significant difference in the refractive errors between the CC and SC group ($P = 0.38$). The axial length of the NC group (24.60 ± 1.30 mm) was significantly shorter than that of the CC (25.74 ± 1.35 mm; $P < 0.001$) and SC groups (25.90 ± 1.38 mm; $P < 0.001$). There was no significant difference in the axial length between the CC and SC groups ($P = 0.95$). The optic disc tilt in the NC group (24.6 ± 11.2 pixels) was significantly less than that in the CC group (38.6 ± 13.6 pixels; $P < 0.001$) and the SC group (48.5 ± 17.3 pixels; $P < 0.001$). And the optic disc tilt in the CC group was significantly less than that in the SC group ($P = 0.02$). The ovality ratio in the NC group (0.96 ± 0.08) was significantly larger than that in the CC group (0.88 ± 0.09; $P = 0.001$) and SC group (0.84 ± 0.13; $P < 0.001$), and the ovality ratio in the CC group was significantly larger than that in the SC group ($P = 0.01$). The PMP was not significantly different among the three groups ($P = 0.07$). The pNFE was more frequently observed in the CC (22/15) and SC groups (31/11) than in the NC group (6/36) but was not significantly different between the CC and SC groups.

Discussion

Our results showed that myopic coni could be detected in 69.0% of the eyes with CC and SC in the color fundus photographs, and two regions could be distinguished in the OCT cross-sectional images. In myopic eye with refractory less than –0.5 D, 78 of 106 eyes (73.6%) had myopic conus. CC was observed in 36 eyes (34.0%), and SC in 42 eyes (39.6%).

Table. Characteristic of Participants

	Non-Conus (42 eyes)	Choroidal Conus (37 eyes)	Scleral Conus (42 eyes)	*P* Value of Kruskal-Wallis or Fisher's Exact Test	*P* Values of Multiple Comparison or Fisher's Exact Test
Age (years)	26.3 ± 4.4	25.6 ± 3.9	25.8 ± 4.0	0.79	
Sex (men/women)	31/11	24/13	27/15	0.61	
Refractive error (diopter)	−2.35 ± 3.38	−5.37 ± 3.00	−6.19 ± 2.53	<0.001	N vs. C <0.001 N vs. S <0.001 C vs. S 0.38
Axial length (mm)	24.60 ± 1.30	25.74 ± 1.35	25.90 ± 1.38	<0.001	N vs. C <0.001 N vs. S <0.001 C vs. S 0.95
Optic disc tilt (pixels)	24.6 ± 11.2	38.6 ± 13.6	48.5 ± 17.3	<0.001	N vs. C <0.001 N vs. S <0.001 C vs. S 0.02
Ovality ratio	0.96 ± 0.08	0.88 ± 0.09	0.84 ± 0.13	<0.001	N vs. C 0.002 N vs. S <0.001 C vs. S 0.01
PMP (degrees)	5.27 ± 3.39	4.86 ± 3.51	6.21 ± 3.15	0.07	
pNFE (yes/no)	6/36	22/15	31/11	<0.001	N vs. C <0.001 N vs. S <0.001 C vs. S 0.23

C, choroidal conus; N, non-conus; PMP, papillomacular position; pNFE, peripapillary nerve fiber elevation; S, scleral conus.

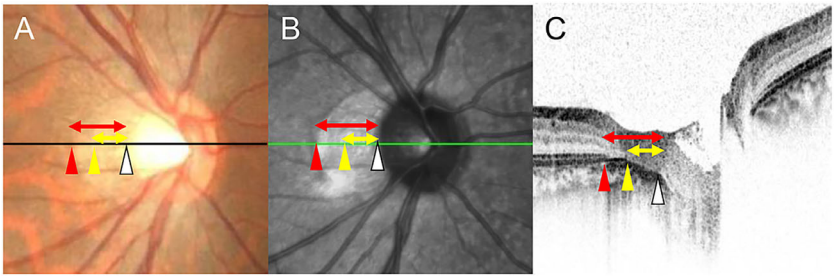

Figure 4. Difference between the classic myopic conus in the fundus photographs and β and γ zone of the PPA. The size of the classically defined conus is shown by the length of the red arrow in the color fundus photograph (A). This corresponds to the end of the elliptical area (red arrow head) to the temporal edge of the optic disc (white arrow head) in the SLO (B) and OCT image (C). Between the red and yellow arrow heads is the beta zone and between the yellow and white arrow heads is the gamma zone (yellow arrow) as defined by Jonas et al.[7] However, the border between beta and gamma zone cannot be seen in the fundus photograph.

In OCT-based definition of SC or CC, the sensitivity of color fundus photograph was 29 of 42 eyes (69.0%) and the specificity was 37 of 37 eyes (100%).The two regions were classified into CC and SC. There were 42 eyes (34.7%) without a myopic conus, and 79 eyes (65.3%) with a myopic conus. In all 79 eyes with a conus, an SC was detected in 42 eyes (53%). Our analyses showed that the eyes with conus had longer axial length and more frequent pNFE than the eyes without conus. In addition, the optic disc was more tilted and elliptical in eyes with an SC than in eyes with only a CC.

The area corresponding to the conus was found to extend from the edge of the ellipsoid zone to the margin of the optic disc. In the area of conus, the OCT measuring light reached the deep layers of the sclera where the brightness of the images was higher than other area (Figs. 1, 2, 4). In the area of the ellipse zone, the OCT measuring light was absorbed by the tissues of the ellipsoid zone, which corresponded with the photoreceptor layer. In the area of the conus, the measuring light reached the sclera owing to the lack of the tissues in the ellipsoid zone. As a result, the white sclera is reflected and the color tone in the conus appears whiter than the surrounding areas by ophthalmoscopy and in the color fundus photographs. The CC appears brownish and the SC appears whitish (Figs. 1, 2, 4) in ophthalmoscopy and in the color fundus photographs. The brown color is owing to the choroidal pigmentation in the CC, and the white color is owing to the white sclera.

Examinations of the OCT images showed that all eyes could be classified as having a CC and/or an SC. However, the two types of coni could not be easily identified in the fundus photographs and the SLO images in 21.4% of the eyes with CC and SC. The reason for this might be that there were some cases in which the edge of the choroid became thinner gradually, and other cases in which the thickness of the choroid was maintained until just before the edge. In the former case, the edge can be distinguished in the OCT images, but the thickness of the choroid with its brownish

pigments decreases gradually. In general, using color fundus photographs, we are able to recognize the difference of some structures only by color. Thus the boundary between the CC and the SC becomes difficult to identify in the fundus photographs. However, in the latter cases, the choroidal thickness, that is, the choroidal brownish pigments, ends abruptly, which enable us to identify the border between CC and SC. This fundamental limitation of the color fundus photographs should be considered to interpret this study.

The eyes with conus tended to have longer axial length, are more myopic, have larger optic disc tilt, smaller ovality ratio, and more frequent pNFE than the eyes without conus. The eyes with both types of coni (SC group) tended to have a larger optic disc tilt and smaller ovality ratio than the eyes with only a CC (CC group). Because an eye with an SC always had a CC, we suggest that the CC develops first, then the SC develops. According to the results of previous studies, a conus occurs from a part of the optic disc associated with an optic disc tilt during the lengthening of the axial length.[15–17] Therefore it is natural that the optic papilla is more tilted and more oval in the eyes with both CC and SC than in eyes with only a CC.

Although juvenile-onset myopia is thought to be characterized by an elongation of the axial length relative to the anterior refracting elements of the eye, the axial length was not different between the CC group and SC group. Our previous study showed that there were myopic changes even in the eyes with short axial lengths, suggesting that the myopic changes are partly dependent on the nonuniform growth of the posterior segment, such as an oval extension of the eye and local enlargements, such as by a posterior staphyloma.[18] This suggests that it is necessary to evaluate the myopic changes in the ocular fundus not only by the axial length but by these other factors.

Eyes with pNFE have higher myopia, longer axial length, and greater optic disc tilt than eyes with no pNFE. Thus the pNFE is a characteristic finding of myopia.[14] The pNFE was observed more frequently in the CC and SC groups than in the NC group. However, there was no significant difference in the incidence of pNFE between the CC and SC groups. Because there were no eyes with only an SC, we suggest that a conus develops primary as a CC followed by the development of an SC. Thus the proportion of eyes with a pNFE should be more frequent in eyes with an SC. However, this was not the case. This suggests that a pNFE occurs mainly while the CC develops but not when the SC develops. Only the sclera is stretched during the development of the SC, whereas the retina and choroid are stretched during the development of the CC. Thus the pNFE, which is induced by the ocular elongation, might less likely occur during the development of the SC.

Earlier studies attempted to match the development of a conus to the PPA in the fundus photographs and that in the OCT images.[19] There were two difficulties with this method. One difficulty was that some of the funduscopic findings, such as the color of the optic disc and conus, cannot be detected by OCT. Also, some of the OCT findings, such as the BM opening and the scleral edge, cannot be detected in the fundus photograph.[20,21] A second problem was the age of the participants. A conus is caused by a stretching of the eye during its elongation. However, the PPA is caused by pathological changes and aging. The older population have both a conus and a PPA. As a result, we could not separate the myopic conus, aging PPA, and pathologic PPA.

We examined the relationship of the conus detected in the fundus photographs and the PPA from previous reports. The conus determined in the color fundus photographs includes the β zone (with BM and without the ellipsoid zone) and γ zone (without BM) of the PPA.[7] However, the border between β and γ zones cannot be seen in the fundus photographs (Fig. 4). We wanted to determine the myopic changes of the ophthalmoscopic conus and studied only young healthy eyes that did not have aging and pathological effects. We found that the conus observed ophthalmoscopically was clearly judged by the edge of the ellipsoid zone, and the ophthalmoscopic border within the conus was the edge of the choroid. However, the other structures, such as the BM and RPE layer, were not visible in the fundus photographs.[20,21] These findings suggest that the edge of the ellipsoid zone and occasionally the choroid can be seen but the edges of the BM and RPE are not seen in the fundus photographs. It is possible that the lateral edge of conus corresponds to the edge of the RPE layer because the brownish tone of color, which would be originated from the RPE layer, changes at the lateral edge of conus in color fundus photograph. However, this cannot always be confirmed by the OCT because the OCT reflectivity of the layers, such as RPE and BM within the conus, is usually enhanced owing to the lack of sensory retina. Thus it is difficult to distinguish between the RPE layer and BM without the RPE layer. This is a limitation of the present method.

This study has limitations. First, the study population was made up of young Japanese volunteers who are known to belong to the most myopic group in the world.[22] Thus our results describe the characteristics of young myopic eyes, but might not necessarily hold for older and nonmyopic populations. However, the reliability of the examination was very high because no pathological factors, such as cataracts or vitreal opacities, were present in these young healthy individuals and their understanding of the purpose of the examinations was high. Second, the narrow range of age prevented an interference by the cohort effects and aging effects. An epidemiologic study should help generalize the present results to other populations. Third, we used the images with the scale of 1:1 pixel, which is a default setting in most of the OCT machines. The error occurs when measuring lengths and angles in OCT images with spatial aspect ratios other than 1:1 micrometer.[23,24] However, it was difficult to detect the borders of CC and SC in the images with the scale of 1:1 micrometer. Thus we used images with the scale of 1:1 pixel in this study. Because we did not analyze the distance and angle in this study, the earlier described problem in the images with the scale of 1:1 pixel were thought to be limited.

Conclusions

Outer border of the conus was the end of the ellipsoid zone in all eyes with an ophthalmoscopic conus. The funduscopic conus was clearly divided into a CC and an SC in the OCT images, but not in the color fundus photographs or the SLO images. The eyes with SC tend to have larger optic disc tilt, smaller ovality ratio, and larger PMP angle than the eyes with a CC only. These findings should be considered when assessing conus in normal and glaucomatous eyes.

Acknowledgments

The authors thank Duco Hamasaki, PhD, of the Bascom Palmer Eye Institute of the University of Miami for providing critical discussions and suggestions to our study and revision of the final manuscript.

Disclosure: **H. Terasaki,** None; **T. Yamashita,** None; **M. Tanaka,** None; **K. Nakao,** None; **T. Sakamoto,** None

References

1. Foster PJ, Oen FT, Machin D, et al. The prevalence of glaucoma in Chinese residents of Singapore: a cross-sectional population survey of the Tanjong Pagar district. *Arch Ophthal*. 2000;118:1105–1111.
2. Rahi JS, Cumberland PM, Peckham CS. Myopia over the lifecourse: prevalence and early life influences in the 1958 British birth cohort. *Ophthalmology*. 2011;118:797–804.
3. Hayashi K, Ohno-Matsui K, Shimada N, et al. Long-term pattern of progression of myopic maculopathy: a natural history study. *Ophthalmology*. 2010;117:1595–1611, 1611.e1–4.
4. Jonas JB, Aung T, Bourne RR, Bron AM, Ritch R, Panda-Jonas S. Glaucoma. *Lancet*. 2017;390:2183–2193.
5. Suzuki Y, Iwase A, Araie M, et al. Risk factors for open-angle glaucoma in a Japanese population: the Tajimi Study. *Ophthalmology*. 2006;113:1613–1617.
6. Morgan IG, Ohno-Matsui K, Saw SM. Myopia. *Lancet*. 2012;379:1739–1748.
7. Jonas JB, Jonas SB, Jonas RA, et al. Parapapillary atrophy: histological gamma zone and delta zone. *PloS One*. 2012;7:e47237.
8. Dai Y, Jonas JB, Huang H, Wang M, Sun X. Microstructure of parapapillary atrophy: beta zone and gamma zone. *Invest Ophthalmol Vis Sci*. 2013;54:2013–2018.
9. Yamada H, Akagi T, Nakanishi H, et al. Microstructure of peripapillary atrophy and subsequent visual field progression in treated primary open-angle glaucoma. *Ophthalmology*. 2016;123:542–551.
10. Sawada Y, Araie M, Shibata H, Ishikawa M, Iwata T, Yoshitomi T. Optic disc margin anatomic features in myopic eyes with glaucoma with spectral-domain OCT. *Ophthalmology*. 2018;125:1886–1897.
11. Tokoro T, Ohno K. *Kinshi Kiso to Rinsho [Myopia Basis and Clinic]*. Bunkyo-ku, Tokyo: Kanehara & Co., Ltd.; 2012:39–45.
12. Garway-Heath DF, Poinoosawmy D, Fitzke FW, Hitchings RA. Mapping the visual field to the optic disc in normal tension glaucoma eyes. *Ophthalmology*. 2000;107:1809–1815.
13. Yamashita T, Sakamoto T, Yoshihara N, et al. Circumpapillary course of retinal pigment epithelium can be fit to sine wave and amplitude of sine wave is significantly correlated with ovality ratio of optic disc. *PloS One*. 2015;10:e0122191.
14. Yamashita T, Sakamoto T, Yoshihara N, et al. Peripapillary nerve fiber elevation in young healthy eyes. *Invest Ophthalmol Vis Sci*. 2016;57:4368–4372.
15. Guo Y, Liu LJ, Tang P, et al. Parapapillary gamma zone and progression of myopia in school children: the Beijing children eye study. *Invest Ophthalmol Vis Sci*. 2018;59:1609–1616.
16. Kim M, Choung HK, Lee KM, Oh S, Kim SH. Longitudinal changes of optic nerve head and peripapillary structure during childhood myopia progression on OCT: Boramae myopia cohort study report 1. *Ophthalmology*. 2018;125:1215–1223.
17. Kim TW, Kim M, Weinreb RN, Woo SJ, Park KH, Hwang JM. Optic disc change with incipient myopia of childhood. *Ophthalmology*. 2012;119:21–26.e1–3.
18. Yamashita T, Sakamoto T, Terasaki H, Tanaka M, Kii Y, Nakao K. Quantification of retinal nerve fiber and retinal artery trajectories using second-order polynomial equation and its association with axial length. *Invest Ophthalmol Vis Sci*. 2014;55:5176–5182.
19. Jonas JB, Jonas SB, Jonas RA, Holbach L, Panda-Jonas S. Histology of the parapapillary region in high myopia. *Am J Ophthalmol*. 2011;152:1021–1029.
20. Chauhan BC, Burgoyne CF. From clinical examination of the optic disc to clinical assessment of the optic nerve head: a paradigm change. *Am J Ophthalmol*. 2013;156:218–227.e2.
21. Chauhan BC, O'Leary N, Almobarak FA, et al. Enhanced detection of open-angle glaucoma with an anatomically accurate optical coherence tomography-derived neuroretinal rim parameter. *Ophthalmology*. 2013;120:535–543.
22. Iwase A, Suzuki Y, Araie M, et al. The prevalence of primary open-angle glaucoma in Japanese: the Tajimi Study. *Ophthalmology*. 2004;111:1641–1648.
23. Kim JH, Kang SW, Ha HS, Kim SJ, Kim JR. Overestimation of subfoveal choroidal thickness by measurement based on horizontally compressed optical coherence tomography images. *Graefes Arch Clin Exp Ophthalmol*. 2012;251:1091–1096.
24. Sigal IA, Schuman JS, Ishikawa H, Kagemann L, Wollstein G. A problem of proportions in OCT-based morphometry and a proposed solution. *Invest Ophthalmol Vis Sci*. 2016;57:484–485.

Investigative Ophthalmology & Visual Science